Carbohydrate Polymers 90 (2012) 261–269

Contents lists available at SciVerse ScienceDirect

Carbohydrate Polymers

journal homepage: www.elsevier.com/locate/carbpol

Facile synthesis of carboxymethyl curdlan-capped silver nanoparticles and their application in SERS

Juan Wu, Fei Zhang, Hongbin Zhang*

Advanced Rheology Institute, Department of Polymer Science and Engineering, School of Chemistry and Chemical Technology, Shanghai Jiao Tong University, Shanghai 200240, China

ARTICLE INFO

Article history:
Received 14 January 2012
Received in revised form 2 April 2012
Accepted 1 May 2012
Available online 17 May 2012

Keywords:
Silver nanoparticle
Carboxymethyl curdlan
UV irradiation
Surface enhanced Raman scattering

ABSTRACT

Carboxymethyl curdlan (CMc), a β-D-glucan derivative, was used in the photoinduced synthesis of Ag nanoparticles. The size, size distribution, morphology and structure of the as-prepared Ag nanoparticles were investigated with UV–vis spectroscopy, transmission electron microscopy (TEM), energy-dispersive X-ray spectrometry (EDX), X-ray diffraction (XRD) and Fourier transform infrared (FTIR) spectroscopy. The experimental results indicated that the particle size increased and the size distribution became broader with increasing the concentrations of both $AgNO_3$ and CMc, and the effect of the latter was more pronounced. With the CMc concentration increasing, the diversity of morphology was obtained as a result of the plasmon excitation and the role of CMc. It was found that CMc played an important role in the synthesis and stabilization of Ag nanoparticles through a series of contrastive experiments. The enhancement effect of the produced Ag nanoparticles in surface enhanced Raman scattering (SERS) was also investigated.

1. Introduction

Currently, metal nanoparticles such as gold and silver have drawn immense attention due to their potential applications as catalyst, optoelectronic nanodevices, substrate for surface-enhanced Raman spectroscopy (SERS), chemical and biological sensors and biomedicine materials (Millstone, Hurst, Métraux, Cutler, & Mirkin, 2009). Concerning the synthesis of metal nanoparticles, especially silver nanoparticles, numerous methods such as chemical reduction (Murphy & Jana, 2002), thermal reduction (Leung, Wong, & Xie, 2010), electrochemical reduction (Rodríguez-Sánchez, Blanco, & López-Quintela, 2000), and other reductions by microwave (Chen, Wang, Zhang, & Jin, 2008; Li et al., 2011), ultrasonic (Jiang et al., 2004; Li, Cai, Li, Hu, & Liu, 2006), γ-ray irradiation (Yoksan & Chirachanchai, 2009), UV irradiation (Zhang, Xu, & Kumacheva, 2005) and templates (Sun, Wiley, Li, & Xia, 2004), have been reported in the literatures. Among them, the most common approach is chemical reduction using sodium borohydride and citrate as the reductant and protection agent respectively to fabricate silver nanoparticles (Cui et al., 2008). The size and shape of Ag nanoparticles are extremely important due to their effects on the physical and chemical properties. A variety of Ag nanoparticles with different shapes such as nanoprisms (Dong et al., 2010; Jin et al., 2003; Jin et al., 2001; Millstone, Wei, Jones, Yoo, & Mirkin, 2008; Xue & Mirkin, 2007; Xue, Meĭtraux, Millstone, & Mirkin, 2008), nanorods (Millstone et al., 2008; Murphy & Jana, 2002), nanowires (Murphy & Jana, 2002; Sun & Xia, 1991; Sun, Yin, Mayers, Herricks, & Xia, 2002) and nanocubes (Sun et al., 2004; Sun & Xia, 2002; Yu & Yam, 2004) have been successfully prepared to explore the shape dependant optical and electronic properties. These different nanostructures can be synthesized in hard or soft templates, which always refer to alumina membrane (Murphy & Jana, 2002), mesoporous silica (Fukuoka et al., 2001), surfactants (Murphy & Jana, 2002; Yu & Yam, 2004), poly-(vinylpyrrolidone) (PVP) (Jiang et al., 2004; Sun & Xia, 2002), polyelectrolyte capsules (Shang & Dong, 2008; Shchukin, Radtchenko, & Sukhorukov, 2003) and dendrimers (Zheng & Dickson, 2002). The majority of reactions are thermally driven, but light-driven reactions are one of the most effective methods for making anisotropic silver nanostructures with controlled size and shape. Photoinduced growth, which was first proposed by Mirkin's group in 2001 (Jin et al., 2001), has been proved to be an efficient way to synthesize nanoprisms. In this method, small spherical seeds were firstly reduced by sodium borohydride, and then subjected to light irradiation and transformed into triangular prisms. The particle size and shape can be controlled by adjusting the wavelength of incident light (Jin et al., 2003; Zheng et al., 2007). This approach suggests a new way of growth of nanoparticles in aqueous solution and the obtained structures

* Corresponding author. Tel.: +86 21 54745005; fax: +86 21 54741297.
E-mail address: hbzhang@sjtu.edu.cn (H. Zhang).

0144-8617/$ – see front matter © 2012 Elsevier Ltd. All rights reserved.
http://dx.doi.org/10.1016/j.carbpol.2012.05.033

can get precise control. However, this method needs preparation of seeds through chemical reduction by sodium borohydride, and the final fabrication involves multiple steps.

For those commonly chemical routes, although they are more available for reduction purposes, the use of toxic chemical reductants such as hydrazine (Zhang, Qiao, Chen, & Wang, 2006), sodium borohydride (Jin et al., 2003; Jin et al., 2001; Murphy & Jana, 2002), DMF (Jiang et al., 2004; Pastoriza-Santos & Liz-Marzán, 2002) etc., poses potential environmental and biological risks. Since the topic of green chemistry and chemical processes was proposed, some biomacromolecules have been introduced as environmentally friendly reducing and capping agents for the synthesis of metal nanoparticles. For example, metal nanoparticles stabilized by DNA (Molotsky, Tamarin, Moshe, Markovich, & Kotlyar, 2011; Petty, Zheng, Nicholas, & Dickson, 2004; Richards et al., 2008) and proteins (McMillan et al., 2002; Templeton, Chen, Gross, & Murray, 1999) have already been extensively studied. Due to the abundant hydroxyl groups present in polysaccharides, preparations of metal nanoparticles by polysaccharides have been also well documented. Raveendran et al. (Raveendran, Fu, & Wallen, 2003; Raveendran, Fu, & Wallen, 2005) firstly reported the completely green synthesis of Ag, Au, and alloy nanoparticles by using β-D-glucose as the reducing agent and starch as a capping agent in aqueous solutions. Furthermore, some other polysaccharides including cyclodextrin (Huang, Meng, & Qi, 2009; Sylvestre, Kabashin, Sacher, Meunier, & Luong, 2004), chitosan (Yoksan & Chirachanchai, 2009; Zhuang, Cheng, Kang, & Xu, 2010), alginate (Gao, Ding, Zheng, Cheng, & Peng, 2007; Saha et al., 2009), cellulose (Cai, Kimura, Wada, & Kuga, 2008; Li et al., 2011), carboxymethyl cellulose (Hebeish, El-Rafie, Abdel-Mohdy, Abdel-Halim, & Emam, 2010; Liu, He, Durham, Zhao, & Roberts, 2008), hyaluronan and heparin (Cui et al., 2008; Xia, Cai, Jiang, & Yao, 2011; Zhang, Wu, & Zhang, 2012), have been also successfully used as reducing agent or capping agent for preparation of metal nanoparticles.

Curdlan is a naturally linear polysaccharide composed of 1, 3-β-D-glucan, which can form physical hydrogels by various methods and has been widely used in foods, pharmaceutical and cosmetic applications (Harada, Terasaki, & Harada, 1993; Nishinari, Zhang, & Funami, 2009). However, curdlan is insoluble in water, which limits its biological applications. Carboxymethyl substitution is considered as an effective method to improve the water-solubility of curdlan. After carboxymethylation, Carboxymethyl curdlan (CMc) has good water solubility as well as antitumor and immunological activities (Jin, Zhang, Yin, & Nishinari, 2006; Ohya, Nishimoto, Murata, & Ouchi, 1994; Sasaki, Abiko, Nitta, Takasuka, & Sugino, 1979). In addition, CMc still has abundant hydroxyl groups in its units, and in neutral solution, CMc possesses negatively charged carboxyl groups, which should make CMc function as a reducing agent or a capping agent as many other polysaccharides did. So, the as-prepared Ag nanoparticles induced by CMc provide great potential for biomedical applications.

A recent paper did report the preparation of Ag nanoparticles stabilized by CMc, in which Ag nanoparticles were synthesized through heating the solution of CMc and $AgNO_3$ at an elevated temperature of 100 °C (Leung et al., 2010). In this work, we proposed a facile synthesis of Ag nanoparticles by UV irradiation of the solution of CMc and $AgNO_3$ without heat treatment. The role of CMc and the effect of concentrations of both Ag ion and CMc on the formation of Ag nanoparticles were studied by UV–vis spectroscopy, transmission electron microscopy (TEM), energy-dispersive X-ray spectrometry (EDX), X-ray diffraction (XRD) and Fourier transform infrared spectroscopy (FTIR). The SERS sensitivity of the obtained Ag nanoparticles was also explored. The overall work addresses a simple and green method to fabricate Ag nanoparticles by one step with SERS sensitivity.

2. Experimental

2.1. Materials

Curdlan was obtained from Takeda-Kirin Foods Corporation (Tokyo, Japan). Carboxymethyl curdlan (CMc) was synthesized by the method described by Sasaki (Sasaki, Abiko, Sugino, & Nitta, 1978). The degree of substitution (DS) of CMc was 0.81 units of carboxymethyl group per one glucose unit in curdlan, determined by conductometric back titration in accordance with a previous report (Eyler, Klug, & Diephuis, 1947). The products obtained were characterized by Fourier transform infrared (FTIR) spectrum and 1H NMR as described in our previous work (Jin et al., 2006) to confirm the successful carboxymethylation. The molecular weight and its distribution of CMc were 6.3×10^5 and 1.55, respectively, measured by Viscotek GPC (Viscotek 270max, Malvern Instruments Ltd., UK). All other reagents were of analytical grade. All solutions were prepared by distilled water.

2.2. Synthesis of silver nanoparticles

To synthesize the Ag nanoparticles, 1 ml of 10 mM $AgNO_3$ solution was added to a certain volume of 1 mg/ml CMc aqueous solution under stirring, and the final volume was adjusted to 5 ml by adding distilled water. The mixing solution was vigorously stirred for 1 h in the dark, and then was irradiated with a conventional UV lamp at $\lambda = 365$ nm (Shanghai Yuying Industrial Co., China, ZF7, 12W) for various exposure time under quiescent conditions.

2.3. Characterization

The size and morphology of as-prepared Ag nanoparticles were characterized by transmission electron microscopy (TEM, JEM-2100, JEOL Ltd., Japan, 200 kV). Energy-dispersive X-ray spectroscopy (EDX) attached to JEM-2100 microscopy was used to determine the elemental composition of the nanoparticles. Absorption spectra were recorded by a UV–vis spectrophotometer (UV-2450, Shimadzu, Japan). Fourier transform infrared (FTIR) spectra were collected in transmittance mode on a FTIR instrument (Spectrum 100, Perkin Elmer, Inc., USA) in the region of 400–4000 cm^{-1}. The crystal structure of product was characterized by wide-angle X-ray diffraction (XRD, D/max-2200/PC, Japan Rigaku Co.). The XRD patterns with Cu Kα radiation ($\lambda = 0.15406$ nm) at 40 kV and 30 mA were recorded in the region of 2θ from 10 to 80° with a step speed of 5°/min. Zeta potential was determined by a Zetasizer90 (ZS90, Malvern Instruments Ltd., UK) and taken as a mean value from three measurements. The pH values were measured by a PHS-3C pH meter with a Combination Electrode (E-201-C, Shanghai Shengci Instrument Co.).

Surface-enhanced Raman measurements were conducted with a Raman imaging microscope (LabRam-1B, Jobin Yvon Inc., NJ) equipped with a He-Ne laser (632.8 nm, 4.3 mW). The reaction solutions prepared from different concentrations of Ag ions were tested.

3. Results and discussion

3.1. Photoinduced formation and characterization of silver nanoparticles

Photoirradiation, which has been proved to be an effective and facile method for preparing Ag nanoparticles, was adopted in the present study. Successful preparation of Ag nanoparticles was shown in Fig. 1. CMc exhibited a strong ability to absorb metallic cations because of abundant carboxyl and hydroxyl groups on its backbone. Photoinduced reduction of $AgNO_3$/CMc without other reductants readily caused apparent formation of Ag nanoparticles,

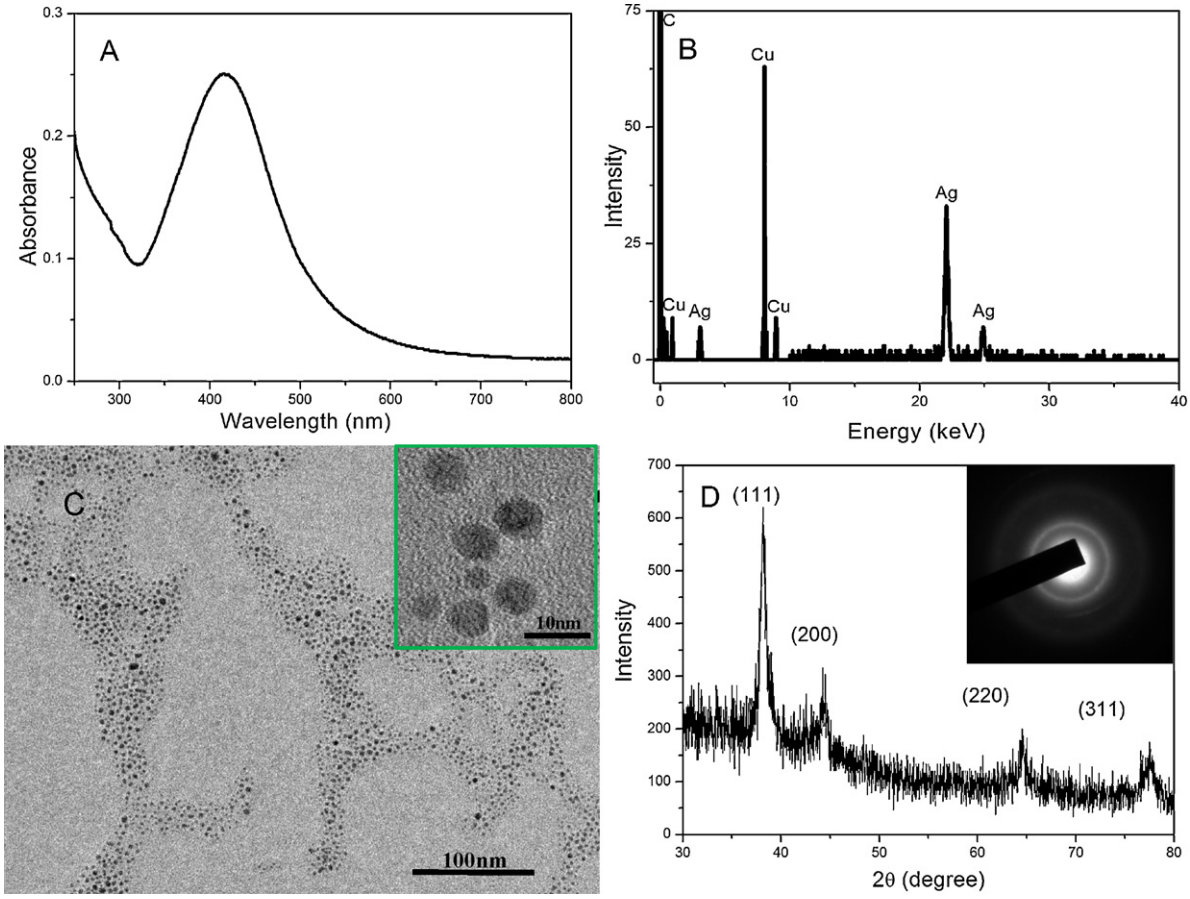

Fig. 1. (A) UV–vis absorption and (B) EDX spectra of Ag nanoparticles prepared by 0.01 mg/ml CMc and 2 mM $AgNO_3$, and the corresponding (C) TEM image and (D) XRD pattern. The inset in C is the high-magnification TEM image. The inset in D is the selected-area electron diffraction pattern of the Ag nanoparticles.

which could be either visually recognized by the color changes of reaction solutions, from transparent to pink, yellow and brown, or verified by UV–vis absorption spectra. As shown in Fig. 1A, it was the UV–vis absorption spectrum of Ag dispersion prepared by the mixing solution of 2 mM $AgNO_3$ and 0.01 mg/ml CMc after 24 h UV-irradiation, in which the absorption peak at about 416 nm is the characteristic surface plasmon resonance of Ag nanoparticles. The apparent formation of Ag nanoparticles was further confirmed by the compositions shown in the EDX spectrum (Fig. 1B) that was used to determine the elemental composition of the nanoparticles. The EDX spectrum displayed strong peaks for Ag, while no signal for Cl atom was detected. Thus, it was conclusive that these nanoparticles were composed of simple substance of Ag. Although the CMc concentration was extreme low, 0.01 mg/ml, CMc could still stabilize the as-prepared Ag nanoparticles and there were no precipitation in two months, similar to Xie's report (Leung et al., 2010), in which they stabilized Ag nanoparticles by 0.01 mg/ml CMc. So, the stabilizing efficiency of CMc for Ag nanoparticles is high.

To investigate the morphology and crystalline structure of Ag nanoparticles, the reaction solution after 24 h UV irradiation were further analyzed by TEM and XRD (Fig. 1C and D). As shown in Fig. 1C, the nanoparticles were almost sphere and their sizes were uniform at about 8 nm. These nanoparticles were also analyzed by electron diffraction directly on the microscope. The selected-area electron diffraction pattern (inset panels in Fig. 1D) showed concentric circles resulted from the orientation of Ag crystal planes. For the crystalline structure of Ag nanoparticles, four peaks can be observed in the XRD spectrum (Fig. 1D), corresponding to diffractions from the (1 1 1), (2 0 0), (2 2 0), and (3 1 1) planes of face-centered-cubic (fcc) phase, respectively (Liu et al., 2008).

The changes of visible colors and UV–vis absorption spectra of the resulting Ag dispersions prepared by various concentrations of $AgNO_3$ and CMc strongly indicated that the size and size distribution of Ag nanoparticles were affected by both the concentrations of $AgNO_3$ and CMc. The effect of concentrations of $AgNO_3$ and CMc solution was explored as follows.

3.2. *Effect of the concentrations of CMc*

Fig. 2 showed the plasmon absorption of Ag nanoparticles that varied with the concentration of CMc. When the concentration of CMc increased from 0.01 mg/ml to 0.5 mg/ml, the intensity of the absorption increased and then decreased, which is likely caused by the decrease of nanoparticles concentration, owing to the formation of large particles or clusters from as-prepared Ag nanoparticles (Heard, Grieser, Barraclough, & Sanders, 1983; Magdassi, Bassa, Vinetsky, & Kamyshny, 2003). It has been also found that the adsorption of capping agents onto Ag nanoparticles could result in strong damping of the absorption band (Magdassi et al., 2003). In addition, the maximum plasmon absorption red-shifted from 416 to 453 nm (inset in Fig. 2) and the bands became much broader with increasing the concentration of CMc, which suggested the size and size distribution of Ag nanoparticles increased. According to Mie theory, small spherical nanocrystals should exhibit a single surface plasmon band, whereas anisotropic particles should exhibit two or three bands, depending on their shape. Larger particles can exhibit additional bands, corresponding

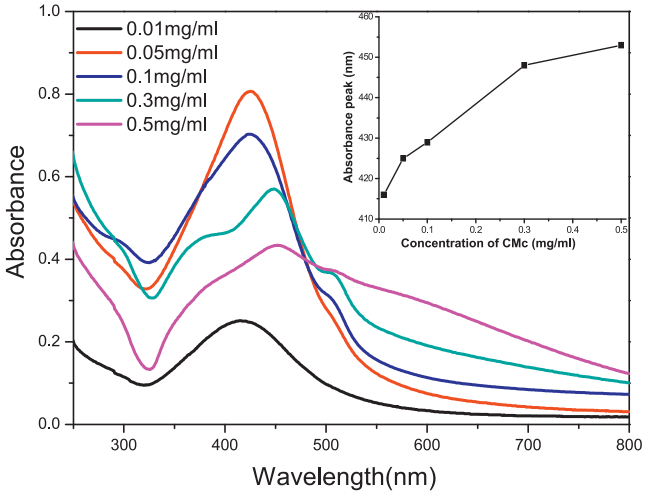

Fig. 2. UV–vis absorption spectra of Ag nanoparticles prepared by 2 mM $AgNO_3$ and CMc at different concentrations (0.01 mg/ml, 0.05 mg/ml, 0.1 mg/ml, 0.3 mg/ml and 0.5 mg/ml). The inset is the trend of maximum absorption peaks.

to quadrupole and higher multiple plasmon excitation (Mie, 1908). In our case, the absorption bands of Ag dispersions stabilized by 0.01 mg/ml and 0.05 mg/ml CMc exhibit unimodal. However, for the systems stabilized by higher concentration of CMc, above 0.1 mg/ml, shoulders centered at 370 and 510 nm were evolved, and especially for the system with 0.5 mg/ml CMc, the absorption band was much broader, which is attributed to the formation of aggregates (Moskovits & Vlčková, 2005) or the deviation from spherical geometry of Ag nanoparticles (Lou, Yuan, & Archer, 2006; Wei & Qian, 2008; Zhang, Langille, & Mirkin, 2010).

The difference in UV–vis absorption suggested the differences in morphology and size distribution of Ag nanoparticles obtained, which could be further confirmed by transmission electron microscopy (TEM) images. Fig. 3 showed the TEM images of Ag nanoparticles prepared by different concentrations of CMc. When the concentration of CMc was 0.05 mg/ml (Fig. 3A), the as-prepared nanoparticles were all spheres and had a uniform size distribution. They were well separated from each other owing to the protection of sufficient CMc molecules, indicating that this concentration of CMc was enough to protect the stabilization of Ag nanoparticles. When the concentration of CMc increased to 0.1 mg/ml, the Ag nanoparticles had a wider size distribution and a larger size of average diameter of 20 nm as shown in Fig. 3B, in which most of the particles were spheres or quasi-spheres, but there still existed some small triangles. These nonspherical particles probably leaded to the evolution of the shoulder centered at 510 nm as evidenced in Fig. 2. Compared to 0.1 mg/ml, the as-prepared nanoparticles stabilized by 0.3 mg/ml CMc were larger in size and dominated by irregular silver particles (Fig. 3C). In addition to spherical nanoparticles, polygonal nanocrystals, such as truncated triangle or hexagon, could be also observed. It has been reported that the plasmon resonance modes for perfect Ag nanoprisms are centered at 340, 470, and 770 nm, which are assigned to out-of-plane quadrupole, in-plane quadrupole, and in-plane dipole resonance, respectively (Jin et al., 2003; Jin et al., 2001). However, if the corners are snipped and truncated, the triangles will become obtuse and a blue-shift will be observed for the corresponding in-plane dipole resonance (Chen & Carroll, 2002; Kelly, Coronado, Zhao, & Schatz, 2002; Millstone et al., 2009; Pastoriza-Santos & Liz-Marzán, 2008). Here, viewed from TEM images, almost all of the triangles were truncated, corresponding well to the result of UV–vis absorption spectra (Fig. 2). As the concentration of CMc increased to 0.5 mg/ml, both the size and size distribution slightly increased (Fig. 3D). The particle morphology had larger diversity and the multiple twined structures were also observed. Kochkar, Aouine, Ghorbel, and Berhault (2011) found that high concentration of β-cyclodextrin favors the formation of multiply twinned particles, in that increase in the β-cyclodextrin concentration restrains the growth of seeds, which hinders the formation of single crystal. It

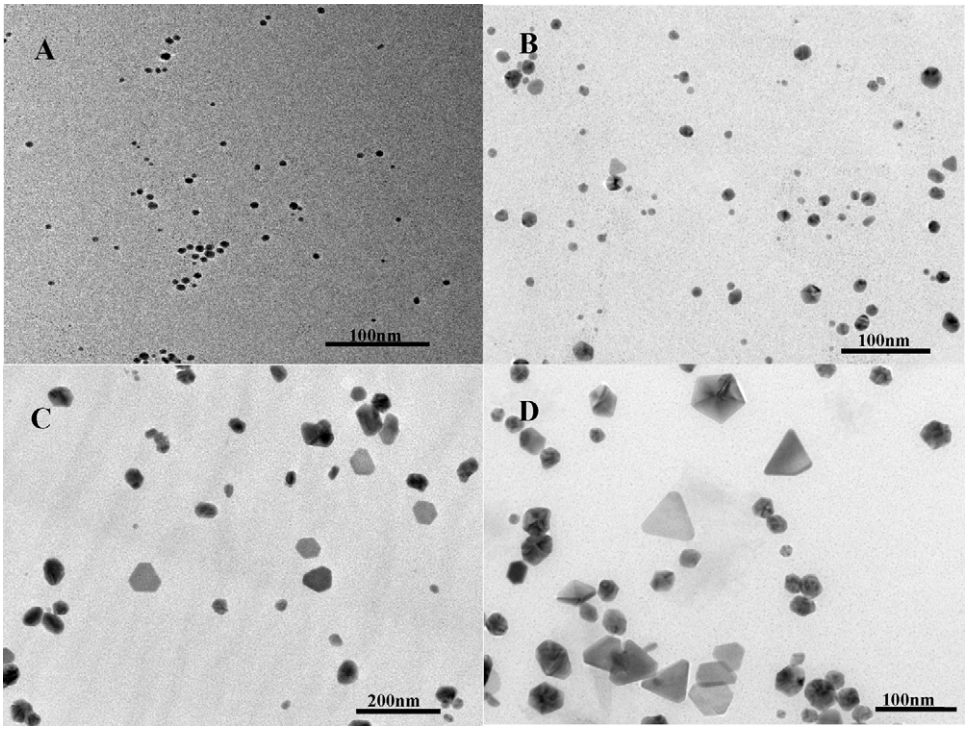

Fig. 3. TEM images of Ag nanoparticles prepared by 2 mM $AgNO_3$ and different concentrations of CMc: (A) 0.05 mg/ml, (B) 0.1 mg/ml, (C) 0.3 mg/ml, and (D) 0.5 mg/ml.

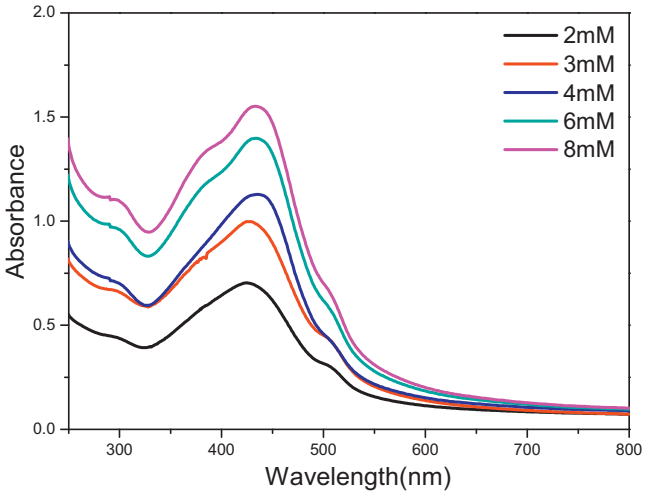

Fig. 4. UV–vis absorption spectra of Ag nanoparticles prepared by 0.1 mg/ml CMc and different concentrations of $AgNO_3$ (2, 3, 4, 6 and 8 mM).

has also been proposed that slow reduction of Ag ions is benefit for twin generation during crystal growth (Xue et al., 2008). Here, the evolution of multiple twined structures with increasing the CMc concentration suggested that the growth rate was slowed down, probably induced by the increase of viscosity of the reaction solution of CMC. When the concentration of CMc increased further, large clusters or aggregations were present and the Ag dispersions destabilized in one week. At high salt concentration, the electrostatic stabilization should be reduced as the Debye length shortens (Wu et al., 2008), leading to the instability of Ag dispersions.

3.3. Effect of the concentration of $AgNO_3$

Fig. 4 showed the UV–vis absorption spectra of Ag nanoparticles prepared by 0.1 mg/ml CMc and different concentrations of $AgNO_3$. When the concentration of $AgNO_3$ was increased from 2 to 8 mM, there was a progressive enhancement for the intensity of the absorption band, which indicated the increased content of Ag nanoparticles in the reaction solution that yielded the high absorbance features. In addition, the maximum plasmon absorption slightly red shifted from 423 to 435 nm following with a broader band, which indicated that the size and size distribution were increased. Weak shoulders at about 510 nm and 370 nm were still existed in UV–vis absorption spectra, which is probably due to the formation of aggregates and nonspherical particles.

These were further confirmed by TEM experiments. The TEM images of Ag nanoparticles prepared with different concentrations of $AgNO_3$ were illustrated in Fig. 5. When the concentration of $AgNO_3$ was increased from 2 to 8 mM, the size of as-prepared Ag nanoparticles increased slightly. Upon increasing the concentration of $AgNO_3$, more nuclei were formed, and relatively few CMc molecules absorbed on the surface of nanoparticles, resulting in the tendency of further growth of Ag nanoparticles. As shown in Fig. 5, although a trace of irregular silver particles was existed, corresponding to the weak shoulders in UV–vis absorption spectra, the particle morphology was almost uniform. High silver concentrations favor the thermal process, which leads to less selectivity for the transformation of isotropic silver seeds into anisotropic triangular prisms (Xue et al., 2008). The effect of the concentration of $AgNO_3$ on particle size and distribution was not so significant in comparison to that of the concentration of CMc.

3.4. The role of CMc in the formation of silver nanoparticles

The above mentioned experimental results strongly suggested that the polydispersity of Ag nanoparticles increased with increasing the concentration of CMc. It is reasonably assumed that CMc plays an important role in the changes in the resulting morphology and size distribution of Ag nanoparticles.

Fig. 6 showed the UV–vis absorption spectra of $AgNO_3$, CMc and their mixing solution before UV irradiation, respectively. Their different patterns verified the interaction between $AgNO_3$ and CMc.

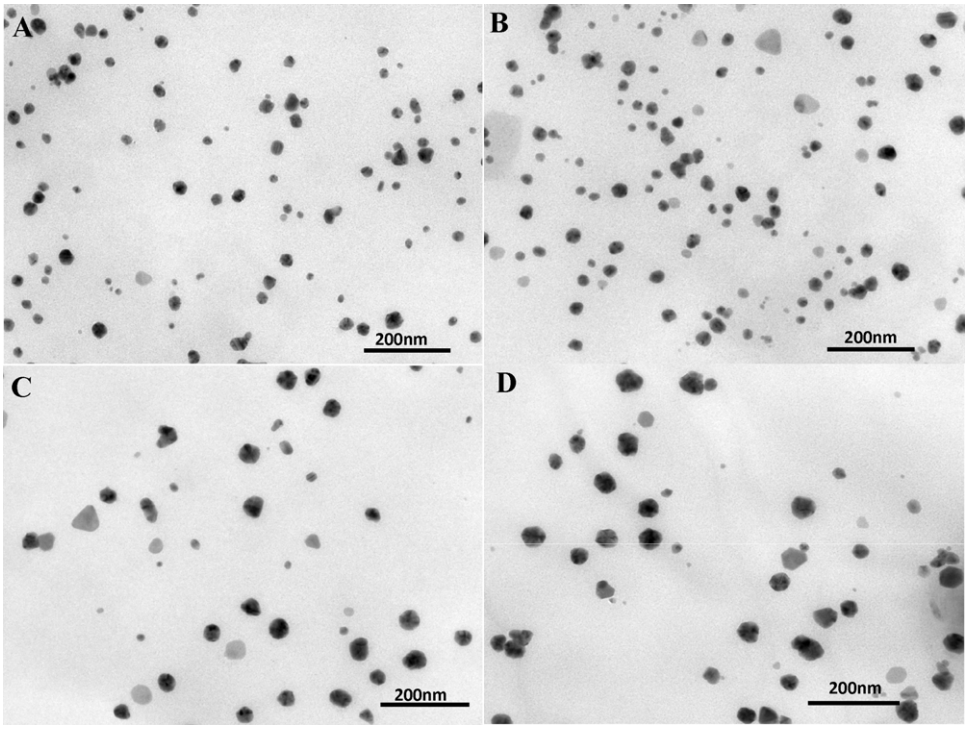

Fig. 5. TEM images of Ag nanoparticles prepared by 0.1 mg/ml CMc and different concentrations of $AgNO_3$: (A) 3 mM, (B) 4 mM, (C) 6 mM, and (D) 8 mM.

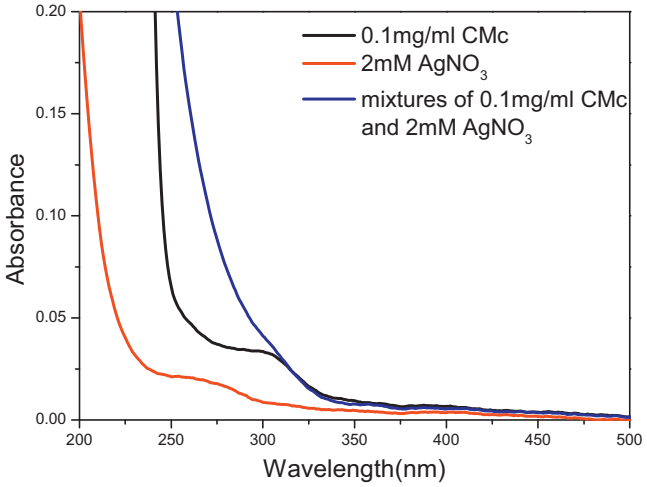

Fig. 6. UV–vis absorption spectra of 2 mM $AgNO_3$, 0.1 mg/ml CMc and their mixing solution before UV irradiation.

When $AgNO_3$ was mixed with CMc solution, Ag ions could bind to CMc macromolecules through carboxyl group chelation, giving rise to the formation of the precursor, CMc-Ag^+, which facilitated the reduction of Ag ions (Xue et al., 2008).

To evaluate the contribution of electrostatic repulsion to the stability of Ag dispersions, the evolution of the zeta potential of Ag dispersions prepared by different concentrations of CMc was investigated (Fig. 7A). The as-prepared Ag nanoparticles all possessed negative charge, indicating that CMc absorbed on the surface of Ag nanoparticles and served as the capping agent to provide electrostatic stabilization for the Ag nanoparticles. The value of zeta potential negatively increased with increasing the concentration of CMc, varying from −22.1 to −40.0 mV, which suggested high concentration of CMc was in favor of the stabilization of Ag nanoparticles. However, the concentration had an upper limit, because large aggregations were present in the Ag dispersions at high salt concentration.

FTIR characterization was used to obtain the more detailed information on the interaction between Ag nanoparticles and CMc molecules, which could be accountable for the reduction of Ag ions and stabilizing Ag nanoparticles. As shown in Fig. 7B, for the IR spectrum of pure CMc powders, the peaks at 1604 and 1427 cm^{-1} were assigned to asymmetric $\nu_{as}(COO^-)$ and symmetric $\nu_s(COO^-)$ stretches, respectively. After lyophilizing the CMc-stabilized Ag dispersion, the IR spectrum of the powers had a new absorption band at 1380 cm^{-1}, and the asymmetric $\nu_{as}(COO^-)$ stretch mode underwent a red shift to 1635 cm^{-1}. A similar IR peak at around 1384 cm^{-1} is considered to be characteristic of carboxylic acids adsorbed on silver and corresponds to the symmetric stretching mode of carboxylate (COO^-) groups (Donati et al., 2009). So, the changes in IR spectra also indicated that CMc molecules interacted with Ag nanoparticles. It has been reported that there are four modes of the interaction between COO^- groups and metal nanoparticles: monodentate, chelating bidentate, bidentate bridging, and ionic interaction (Liu et al., 2008). The wavenumber separation, Δ, between the $\nu_{as}(COO^-)$ and $\nu_s(COO^-)$ bands can be used to diagnose the type of the interaction. The largest Δ (200–320 cm^{-1}) is corresponding to the monodentate interaction and the smallest Δ (<110 cm^{-1}) is for the chelating bidentate, while the medium range Δ (140–190 cm^{-1}) is for the bidentate bridging (Liu et al., 2008). In the present work, the Δ value was 255 cm^{-1} (1635–1380 cm^{-1}), thus, the interaction mode between COO^- groups and Ag nanoparticles belongs to the monodentate interaction. This type of interaction was different from that of COO^- groups in carboxymethyl cellulose (CMC) with Pd Nanoparticles (bidentate bridging) (Liu et al., 2008), which may be due to the different properties of metals. These interactions facilitated the formation and stabilization of Ag nanoparticles.

To identify the capability of CMc in the preparation and stabilization of Ag nanoparticles, a series of control experiments were further carried out: (1) UV irradiation of $AgNO_3$ solution in the absence of CMc; (2) UV irradiation of CMc solution alone; (3) the mixing solution of 0.1 mg/ml CMc and 2 mM $AgNO_3$ was stored in dark at room temperature; and (4) UV irradiation of the mixing solution of 0.1 mg/ml CMc and 2 mM $AgNO_3$, the pH value of which was adjusted to 4. For the former two cases, the final solutions were both colorless and transparent after 24 h UV irradiation, and the UV–vis absorption results showed no characteristics of Ag nanoparticles. However, upon addition of CMc, the color of the reaction solution changed and Ag nanoparticles were formed quickly. It was indicated that the presence of CMc in the reaction solution was vital for the synthesis of Ag nanoparticles under UV irradiation. For the neutral reaction solution stored in dark, no change was observed in three days, showing that CMc could not reduce Ag ions at room temperature without UV irradiation. Mirkin et al. (Xue et al., 2008) also found that the mixture of $AgNO_3$ and citrate is quite stable in the dark for several days. This fact implies that the required activation energy for the reduction reaction of Ag ions should be high, so that in the dark at room temperature CMc could not overcome the energy barrier for conversion of Ag ion to Ag particles. For the last case, black precipitation was obtained in the reaction solution irradiated for 24 h. At pH 4, COO^- groups in CMc molecules turned into COOH groups, which could not stabilize with

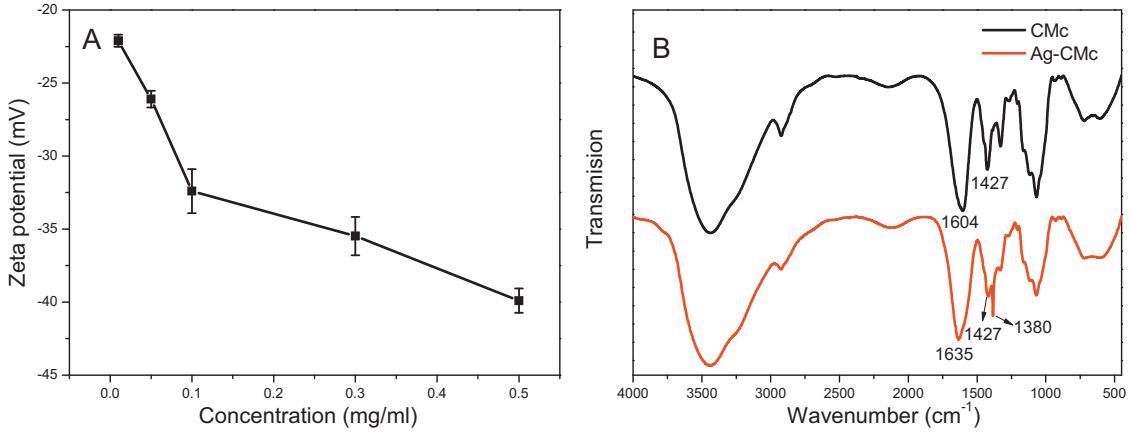

Fig. 7. (A) The trend of zeta potential of Ag dispersions prepared by different concentrations of CMc; (B) FTIR spectra of CMc powder and CMc-stabilized Ag nanoparticles.

Ag nanoparticles. Therefore, the presence of COO^- groups on CMc was vital for the stabilization of nanoparticles. Based on these four control experiments, it was indicated that CMc played an important role in the reduction and stabilization of Ag ions, which should serve as both a redundant under UV irradiation and a stabilizer of Ag nanoparticles.

Considered from the aspect of plasmon excitation, when electrons in silver colloid are excited by incident light, energy is transferred from the incident light to the nanoparticles. The energy absorbed initially generates hot electrons but will quickly disperse through electron-electron scattering and electron-phonon coupling (Pelton, Aizpurua, & Bryant, 2008). However, when the reaction solution contained a capping agent, it is proposed that a charge can transfer between adsorbates and the hot electrons (holes) in nanoparticles resulted from plasmon excitation in the photochemical reaction (Lindstrom & Zhu, 2006; Watanabe, Menzel, Nilius, & Freund, 2006). Mirkin and his coworkers discussed the chemical roles of citrate in the photoreaction. When Ag nanoparticles are excited by incident light, the hot electrons generated on the surfaces of the nanoparticles transfer to the unoccupied orbitals of the adsorbed silver cations. The hot holes are then filled with electrons from the oxidization of adsorbed citrate (decarboxylation of citrate) (Xue et al., 2008). Kochi and co-workers investigated charge-transfer photoactivation of the electron donor-acceptor salts (A^+) with carboxylate donors ($R\text{-}COO^-$), leading to transient radical pairs ($R\text{-}COO^{\bullet}$, $A^{\bullet}$), and real-time monitored the decarboxylation of labile acyloxy radicals ($R\text{-}COO^{\bullet}$) by C—C bond cleavage, producing CO_2. Through femtosecond time-resolved spectroscopy, it is revealed that the decarboxylation rate constant is below $1 \times 10^9\ s^{-1}$ (Bockman, Hubig, & Kochi, 1996).

In the present work, owing to the charge-transfer photoactivation effect, a trace of Ag nanoparticles was possibly formed. The new-formed Ag nanoparticle could further catalyze the process of charge transfer in the intermediate, Ag^+-CMc or Ag^+-CMc-Ag_n, which is facilitated for the further reduction.

For the formation of the silver nanoprisms at high CMc concentrations, it can be explained from the aspect of crystal facet surface energetics (Millstone et al., 2009). As is known already, the (1 1 1), (1 0 0), and (1 1 0) surfaces of face-centered cubic structured metal particles are different, not only in their surface atom densities, but also in their electronic structure, bonding, and possibly chemical reactivities. The surface free energies of these crystallographic planes increased in the order: (1 1 1) > (1 0 0) > (1 1 0), resulting in the bonding abilities and chemical reativities of the (1 1 0) facet being greater than the (1 0 0) and (1 1 1) (Hu et al., 2004). It was also suggested that proteins, organic acids and polysaccharides are expected to interact with the crystal faces differently, thereby changing the surface energies of the latter in due course (Balaji et al., 2009). So, here for the Ag nanoparticles formed in the CMc templates, the interaction was probably directional, leading to the anisotropic growth of Ag nanoparticles under UV irradiation.

It is proposed that slow reduction of Ag ions favors the twin generation during crystal growth (Lofton & Sigmund, 2005; Xiong, Washio, Chen, Sadilek, & Xia, 2007), which is also benefit for the formation of Ag nanoprisms (Xue et al., 2008). However, rapid reduction of Ag ion through a conventionally thermal process usually results in the formation of spherical or pseudospherical particles such as cuboctahedrons and icosahedrons (Lofton & Sigmund, 2005; Xiong et al., 2007). If the photoinduced growth rate is slow and close to the growth rate of the thermal growth process, isotropic growth will be competitive with anisotropic growth, and a broad distribution of product shapes will be observed (Xue et al., 2008). In our study, with increasing the CMc concentration, both the distributions of size and shape became broader, which should be ascribed to the slow photoinduced growth rates approaching to the thermal growth rates.

3.5. Application of Ag nanoparticles in SERS

The application of the as-prepared Ag nanoparticles in SERS was investigated. Fig. 8 showed the SERS spectra of the reaction solutions prepared by different concentrations of $AgNO_3$ in the presence of 0.1 mg/ml CMc. For 0.1 mg/ml CMc solution alone, no obvious peaks could be observed. After irradiation, Ag nanoparticles were created, which chelated with CMc, so their structural information could be detected by Raman spectrum. While only three obvious peaks were detected for 2 mM $AgNO_3$ system, the Raman spectrum of 4 mM $AgNO_3$ system gives a relatively full specification. As shown in Fig. 8, the strong peak at ca. 240 cm^{-1} is attributed to Ag—O stretching vibration (Chang, Ko, Gunawidjaja, & Tsukruk, 2011), corresponding to the interaction between Ag nanoparticles and CMc. The peaks at 1396 cm^{-1} (Fig. 8A) and 1390 cm^{-1} (Fig. 8B) are considered to be characteristic of carboxylic acids adsorbed on silver and corresponds to the symmetric stretching mode of carboxylate groups (Donati et al., 2009; Ivleva, Wagner, Horn, Niessner, & Haisch, 2008). The peaks at 935 cm^{-1} (Fig. 8A) and 930 cm^{-1} (Fig. 8B) belong to C—C skeletal vibration associated with the β linkages (Cui et al., 2008). In Fig. 8A, the peak at 1638 cm^{-1} results from the asymmetric stretching mode of carboxylate groups, the peak at 1297 cm^{-1} is assigned to the C—H deformations, the peak at 1038 cm^{-1} related to C—C, C—O stretch

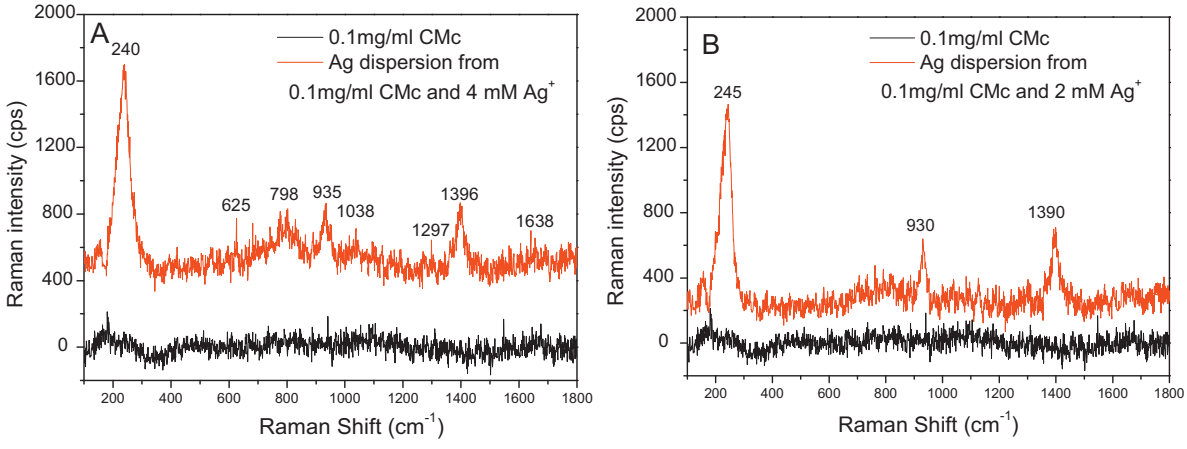

Fig. 8. SERS spectra of the reaction solutions prepared from (A) 4 mM $AgNO_3$ and (B) 2 mM $AgNO_3$ in the presence of 0.1 mg/ml CMc after 24 h UV irradiation. SERS spectrum of 0.1 mg/ml CMc alone was also shown for comparison.

and the peaks at 798 cm^{-1}, 625 cm^{-1} associated with C—O—C glycosidic link vibrations (Ivleva et al., 2008).

The enhancement was attributed to the electromagnetic effects in aggregates combined with either intramolecular or metal-to-molecule resonances (Panigrahi et al., 2006). As mentioned above, the size and size distribution of Ag nanoparticles stabilized by 4 mM $AgNO_3$ were larger than those of Ag nanoparticles stabilized by 2 mM $AgNO_3$. Therefore, it could be concluded that the larger the size, the stronger the SERS intensity.

4. Conclusion

In this work, a green, facile and one-stepped method was used to synthesize Ag nanoparticles under UV irradiation. Carboxymethyl curdlan (CMc) was introduced as a redundant under UV irradiation and a stabilizer of Ag nanoparticles. CMc had a high chelation capacity and good stabilizing efficiency for Ag nanoparticles. The resulting Ag dispersions with low concentration of CMc can keep stable in two month. The size and size distribution of Ag nanoparticles varied with the concentrations of CMc and $AgNO_3$. Dispersions containing spherical and polygonal Ag nanocrystals of truncated triangles or hexagons could be obtained due to the induced role of CMc.

The application of Ag nanoparticles in SERS showed that more Raman scattering peaks could be detected and the peak intensities were enhanced with the increase in $AgNO_3$ concentration that leaded to enlarged Ag particles.

Acknowledgements

The authors are thankful for the financial support for this work from the Shanghai Leading Academic Discipline Project (no. B202).

References

Balaji, D. S., Basavaraja, S., Deshpande, R., Mahesh, D. B., Prabhakar, B. K., & Venkataraman, A. (2009). Extracellular biosynthesis of functionalized silver nanoparticles by strains of Cladosporium cladosporioides fungus. *Colloids and Surfaces B: Biointerfaces*, *68*(1), 88–92.

Bockman, T. M., Hubig, S. M., & Kochi, J. K. (1996). Direct observation of carbon—carbon bond cleavage in ultrafast decarboxylations. *Journal of the American Chemical Society*, *118*(18), 4502–4503.

Cai, J., Kimura, S., Wada, M., & Kuga, S. (2008). Nanoporous cellulose as metal nanoparticles support. *Biomacromolecules*, *10*(1), 87–94.

Chang, S., Ko, H., Gunawidjaja, R., & Tsukruk, V. V. (2011). Raman markers from silver nanowire crossbars. *The Journal of Physical Chemistry C*, *115*(11), 4387–4394.

Chen, S., & Carroll, D. L. (2002). Synthesis and characterization of truncated triangular silver nanoplates. *Nano Letters*, *2*(9), 1003–1007.

Chen, J., Wang, J., Zhang, X., & Jin, Y. (2008). Microwave-assisted green synthesis of silver nanoparticles by carboxymethyl cellulose sodium and silver nitrate. *Materials Chemistry and Physics*, *108*(2–3), 421–424.

Cui, X., Li, C. M., Bao, H., Zheng, X., Zang, J., Ooi, C. P., et al. (2008). Hyaluronan-assisted photoreduction synthesis of silver nanostructures: From nanoparticle to nanoplate. *The Journal of Physical Chemistry C*, *112*(29), 10730–10734.

Donati, I., Travan, A., Pelillo, C., Scarpa, T., Coslovi, A., Bonifacio, A., et al. (2009). Polyol synthesis of silver nanoparticles: Mechanism of reduction by alditol bearing polysaccharides. *Biomacromolecules*, *10*(2), 210–213.

Dong, X., Ji, X., Jing, J., Li, M., Li, J., & Yang, W. (2010). Synthesis of triangular silver nanoprisms by stepwise reduction of sodium borohydride and trisodium citrate. *The Journal of Physical Chemistry C*, *114*(5), 2070–2074.

Eyler, R. W., Klug, E. D., & Diephuis, F. (1947). Determination of degree of substitution of sodium carboxymethylcellulose. *Analytical Chemistry*, *19*(1), 24–27.

Fukuoka, A., Higashimoto, N., Sakamoto, Y., Sasaki, M., Sugimoto, N., Inagaki, S., et al. (2001). Ship-in-bottle synthesis and catalytic performances of platinum carbonyl clusters, nanowires, and nanoparticles in micro-and mesoporous materials. *Catalysis Today*, *66*(1), 23–31.

Gao, Y., Ding, X., Zheng, Z., Cheng, X., & Peng, Y. (2007). *Template-free method to prepare polymer nanocapsules embedded with noble metal nanoparticles. Chemical communications* England: Cambridge., p. 3720.

Harada, T., Terasaki, M., & Harada, A. (1993). Curdlan. In R. L. Whistler, & J. N. BeMiller (Eds.), *Industrial gums* (pp. 427–445).

Heard, S. M., Grieser, F., Barraclough, C. G., & Sanders, J. V. (1983). The characterization of ag sols by electron microscopy, optical absorption, and electrophoresis. *Journal of Colloid and Interface Science*, *93*(2), 545–555.

Hebeish, A. A., El-Rafie, M. H., Abdel-Mohdy, F. A., Abdel-Halim, E. S., & Emam, H. E. (2010). Carboxymethyl cellulose for green synthesis and stabilization of silver nanoparticles. *Carbohydrate Polymers*, *82*(3), 933–941.

Hu, J. Q., Chen, Q., Xie, Z. X., Han, G. B., Wang, R. H., Ren, B., et al. (2004). A Simple and effective route for the synthesis of crystalline silver nanorods and nanowires. *Advanced Functional Materials*, *14*(2), 183–189.

Huang, T., Meng, F., & Qi, L. (2009). Facile synthesis and one-dimensional assembly of cyclodextrin-capped gold nanoparticles and their applications in catalysis and surface-enhanced raman scattering. *The Journal of Physical Chemistry C*, *113*(31), 13636–13642.

Ivleva, N. P., Wagner, M., Horn, H., Niessner, R., & Haisch, C. (2008). In situ surface-enhanced Raman scattering analysis of biofilm. *Analytical Chemistry*, *80*(22), 8538–8544.

Jiang, L.-P., Xu, S., Zhu, J.-M., Zhang, J.-R., Zhu, J.-J., & Chen, H.-Y. (2004). Ultrasonic-assisted synthesis of monodisperse single-crystalline silver nanoplates and gold nanorings. *Inorganic Chemistry*, *43*(19), 5877–5883.

Jin, R., Cao, Y. C., Hao, E., Métraux, G. S., Schatz, G. C., & Mirkin, C. A. (2003). Controlling anisotropic nanoparticle growth through plasmon excitation. *Nature*, *425*(6957), 487–490.

Jin, R., Cao, Y. W., Mirkin, C. A., Kelly, K., Schatz, G. C., & Zheng, J. (2001). Photoinduced conversion of silver nanospheres to nanoprisms. *Science*, *294*(5548), 1901.

Jin, Y., Zhang, H., Yin, Y., & Nishinari, K. (2006). Comparison of curdlan and its carboxymethylated derivative by means of Rheology, DSC, and AFM. *Carbohydrate Research*, *341*(1), 90–99.

Kelly, K. L., Coronado, E., Zhao, L. L., & Schatz, G. C. (2002). The optical properties of metal nanoparticles: The influence of size, shape, and dielectric environment. *The Journal of Physical Chemistry B*, *107*(3), 668–677.

Kochkar, H., Aouine, M., Ghorbel, A., & Berhault, G. (2011). Shape-controlled synthesis of silver and palladium nanoparticles using β-cyclodextrin. *The Journal of Physical Chemistry C*, *115*(23), 11364–11373.

Leung, T. C. Y., Wong, C. K., & Xie, Y. (2010). Green synthesis of silver nanoparticles using biopolymers, carboxymethylated-curdlan and fucoidan. *Materials Chemistry and Physics*, *121*(3), 402–405.

Li, C., Cai, W., Li, Y., Hu, J., & Liu, P. (2006). Ultrasonically induced Au nanoprisms and their size manipulation based on aging. *The Journal of Physical Chemistry B*, *110*(4), 1546–1552.

Li, S.-M., Jia, N., Ma, M.-G., Zhang, Z., Liu, Q.-H., & Sun, R.-C. (2011). Cellulose–silver nanocomposites: Microwave-assisted synthesis, characterization, their thermal stability, and antimicrobial property. *Carbohydrate Polymers*, *86*(2), 441–447.

Lindstrom, C. D., & Zhu, X. Y. (2006). Photoinduced electron transfer at molecule–metal interfaces. *Chemical Reviews*, *106*(10), 4281–4300.

Liu, J., He, F., Durham, E., Zhao, D., & Roberts, C. B. (2008). Polysugar-stabilized Pd nanoparticles exhibiting high catalytic activities for hydrodechlorination of environmentally deleterious trichloroethylene. *Langmuir*, *24*(1), 328–336.

Lofton, C., & Sigmund, W. (2005). Mechanisms controlling crystal habits of gold and silver colloids. *Advanced Functional Materials*, *15*(7), 1197–1208.

Lou, X. W., Yuan, C., & Archer, L. A. (2006). An unusual example of hyperbranched metal nanocrystals and their shape evolution. *Chemistry of Materials*, *18*(17), 3921–3923.

Magdassi, S., Bassa, A., Vinetsky, Y., & Kamyshny, A. (2003). Silver nanoparticles as pigments for water-based ink-jet inks. *Chemistry of Materials*, *15*(11), 2208–2217.

McMillan, R. A., Paavola, C. D., Howard, J., Chan, S. L., Zaluzec, N. J., & Trent, J. D. (2002). Ordered nanoparticle arrays formed on engineered chaperonin protein templates. *Nature Materials*, *1*(4), 247–252.

Mie, G. (1908). Contributions to the optics of turbid media especially colloidal metal solutions. *Annals of Physics*, *25*, 377–452.

Millstone, J. E., Hurst, S. J., Métraux, G. S., Cutler, J. I., & Mirkin, C. A. (2009). Colloidal gold and silver triangular nanoprisms. *Small*, *5*(6), 646–664.

Millstone, J. E., Wei, W., Jones, M. R., Yoo, H., & Mirkin, C. A. (2008). Iodide ions control seed-mediated growth of anisotropic gold nanoparticles. *Nano Letters*, *8*(8), 2526–2529.

Molotsky, T., Tamarin, T., Moshe, A. B., Markovich, G., & Kotlyar, A. B. (2011). Synthesis of chiral silver clusters on a DNA template. *The Journal of Physical Chemistry C*, *114*, 15951–15954.

Moskovits, M., & Vlčková, B. (2005). Adsorbate-induced silver nanoparticle aggregation kinetics. *The Journal of Physical Chemistry B*, *109*(31), 14755–14758.

Murphy, C. J., & Jana, N. R. (2002). Controlling the aspect ratio of inorganic nanorods and nanowires. *Advanced Materials*, *14*(1), 80.

Nishinari, K., Zhang, H., & Funami, T. (2009). *Curdlan*. In P. A. W. G. O Phillips (Ed.), Handbook of hydrocolloids, (pp. 567–591). England.

Ohya, Y., Nishimoto, T., Murata, J., & Ouchi, T. (1994). Immunological enhancement activity of muramyl dipeptide analogue/CM-curdlan conjugate. *Carbohydrate Polymers*, *23*(1), 47–54.

Panigrahi, S., Praharaj, S., Basu, S., Ghosh, S. K., Jana, S., Pande, S., et al. (2006). Self-assembly of silver nanoparticles: Synthesis, stabilization, optical properties, and application in surface-enhanced Raman scattering. *The Journal of Physical Chemistry B*, *110*(27), 13436–13444.

Pastoriza-Santos, I., & Liz-Marzán, L. M. (2002). Synthesis of silver nanoprisms in DMF. *Nano Letters*, *2*(8), 903–905.

Pastoriza-Santos, I., & Liz-Marzán, L. M. (2008). Colloidal silver nanoplates. State of the art and future challenges. *Journal of Materials Chemistry*, *18*(15), 1724–1737.

Pelton, M., Aizpurua, J., & Bryant, G. (2008). Metal-nanoparticle plasmonics. *Laser & Photonics Reviews*, *2*(3), 136–159.

Petty, J. T., Zheng, J., Nicholas, V., & Dickson, R. M. (2004). DNA-templated Ag nanocluster formation. *Journal of the American Chemical Society*, *126*(16), 5207–5212.

Raveendran, P., Fu, J., & Wallen, S. L. (2003). Completely green synthesis and stabilization of metal nanoparticles. *Journal of the American Chemical Society*, *125*(46), 13940–13941.

Raveendran, P., Fu, J., & Wallen, S. L. (2005). A simple and green method for the synthesis of Au, Ag, and Au–Ag alloy nanoparticles. *Green Chemistry*, *8*(1), 34–38.

Richards, C. I., Choi, S., Hsiang, J. C., Antoku, Y., Vosch, T., Bongiorno, A., et al. (2008). Oligonucleotide-stabilized Ag nanocluster fluorophores. *Journal of the American Chemical Society*, *130*(15), 5038–5039.

Rodríguez-Sánchez, L., Blanco, M. C., & López-Quintela, M. A. (2000). Electrochemical synthesis of silver nanoparticles. *The Journal of Physical Chemistry B*, *104*(41), 9683–9688.

Saha, S., Pal, A., Pande, S., Sarkar, S., Panigrahi, S., & Pal, T. (2009). Alginate gel-mediated photochemical growth of mono-and bimetallic gold and silver nanoclusters and their application to surface-enhanced Raman scattering. *The Journal of Physical Chemistry C*, *113*(18), 7553–7560.

Sasaki, T., Abiko, N., Nitta, K., Takasuka, N., & Sugino, Y. (1979). Antitumor activity of carboxymethylglucans obtained by carboxymethylation of (1-3)-[beta]-D-glucan from *Alcaligenes faecalis* var. myxogenes IFO 13140. *European Journal of Cancer (1965)*, *15*(2), 211–215.

Sasaki, T., Abiko, N., Sugino, Y., & Nitta, K. (1978). Dependent on chair length of antitumor activity of (1-3)-beta-D-glucan from Alcaligenes var. faecalis myxogenes IFO 13140 and its acid-degraded productions. *Cancer Research*, *38*, 379–384.

Shang, L., & Dong, S. (2008). Facile preparation of water-soluble fluorescent silver nanoclusters using a polyelectrolyte template. *Chemical Communications*, *9*, 1088–1090.

Shchukin, D. G., Radtchenko, I. L., & Sukhorukov, G. B. (2003). Photoinduced reduction of silver inside microscale polyelectrolyte capsules. *Chemphyschem*, *4*(10), 1101–1103.

Sun, Y., Wiley, B., Li, Z. Y., & Xia, Y. (2004). Synthesis and optical properties of nanorattles and multiple-walled nanoshells/nanotubes made of metal alloys. *Journal of the American Chemical Society*, *126*(30), 9399–9406.

Sun, Y., & Xia, Y. (1991). Large-scale synthesis of uniform silver nanowires through a soft, self-seeding, polyol process. *Nature*, *353*, 737.

Sun, Y., & Xia, Y. (2002). Shape-controlled synthesis of gold and silver nanoparticles. *Science*, *298*(5601), 2176.

Sun, Y., Yin, Y., Mayers, B. T., Herricks, T., & Xia, Y. (2002). Uniform silver nanowires synthesis by reducing $AgNO_3$ with ethylene glycol in the presence of seeds and poly (vinyl pyrrolidone). *Chemistry of Materials*, *14*(11), 4736–4745.

Sylvestre, J. P., Kabashin, A. V., Sacher, E., Meunier, M., & Luong, J. H. T. (2004). Stabilization and size control of gold nanoparticles during laser ablation in aqueous cyclodextrins. *Journal of the American Chemical Society*, *126*(23), 7176–7177.

Templeton, A. C., Chen, S., Gross, S. M., & Murray, R. W. (1999). Water-soluble, isolable gold clusters protected by tiopronin and coenzyme A monolayers. *Langmuir*, *15*(1), 66–76.

Watanabe, K., Menzel, D., Nilius, N., & Freund, H.-J. (2006). Photochemistry on metal nanoparticles. *Chemical Reviews*, *106*(10), 4301–4320.

Wei, D., & Qian, W. (2008). Facile synthesis of Ag and Au nanoparticles utilizing chitosan as a mediator agent. *Colloids and Surfaces B: Biointerfaces*, *62*(1), 136–142.

Wu, X., Redmond, P. L., Liu, H., Chen, Y., Steigerwald, M., & Brus, L. (2008). Photovoltage mechanism for room light conversion of citrate stabilized silver nanocrystal seeds to large nanoprisms. *Journal of the American Chemical Society*, *130*(29), 9500–9506.

Xia, N., Cai, Y., Jiang, T., & Yao, J. (2011). Green synthesis of silver nanoparticles by chemical reduction with hyaluronan. *Carbohydrate Polymers*, *86*(2), 956–961.

Xiong, Y., Washio, I., Chen, J., Sadilek, M., & Xia, Y. (2007). Trimeric clusters of silver in aqueous $AgNO_3$ solutions and their role as nuclei in forming triangular nanoplates of silver. *Angewandte Chemie*, *119*(26), 5005–5009.

Xue, C., Meĭtraux, G. S., Millstone, J. E., & Mirkin, C. A. (2008). Mechanistic study of photomediated triangular silver nanoprism growth. *Journal of the American Chemical Society*, *130*(26), 8337–8344.

Xue, C., & Mirkin, C. A. (2007). pH-Switchable silver nanoprism growth pathways. *Angewandte Chemie International Edition*, *46*(12), 2036–2038.

Yoksan, R., & Chirachanchai, S. (2009). Silver nanoparticles dispersing in chitosan solution: Preparation by [gamma]-ray irradiation and their antimicrobial activities. *Materials Chemistry and Physics*, *115*(1), 296–302.

Yu, D., & Yam, V. W. W. (2004). Controlled synthesis of monodisperse silver nanocubes in water. *Journal of the American Chemical Society*, *126*(41), 13200–13201.

Zhang, F., Wu, J., & Zhang, H. (2012). Construction of hyaluronan-silver nanoparticle – Hemoglobin multilayer composite film and investigations on its electrocatalytic properties. *Journal of Solid State Electrochemistry*, *16*, 1683–1692.

Zhang, J., Langille, M. R., & Mirkin, C. A. (2010). Photomediated synthesis of silver triangular bipyramids and prisms: The effect of pH and BSPP. *Journal of the American Chemical Society*, *132*(35), 12502–12510.

Zhang, J., Xu, S., & Kumacheva, E. (2005). Photogeneration of fluorescent silver nanoclusters in polymer microgels. *Advanced Materials*, *17*(19), 2336–2340.

Zhang, W., Qiao, X., Chen, J., & Wang, H. (2006). Preparation of silver nanoparticles in water-in-oil AOT reverse micelles. *Journal of Colloid and Interface Science*, *302*(1), 370–373.

Zheng, J., & Dickson, R. M. (2002). Individual water-soluble dendrimer-encapsulated silver nanodot fluorescence. *Journal of the American Chemical Society*, *124*(47), 13982–13983.

Zheng, X., Xu, W., Corredor, C., Xu, S., An, J., Zhao, B., et al. (2007). Laser-induced growth of monodisperse silver nanoparticles with tunable surface plasmon resonance properties and a wavelength self-limiting effect. *The Journal of Physical Chemistry C*, *111*(41), 14962–14967.

Zhuang, X., Cheng, B., Kang, W., & Xu, X. (2010). Electrospun chitosan/gelatin nanofibers containing silver nanoparticles. *Carbohydrate Polymers*, *82*(2), 524–527.